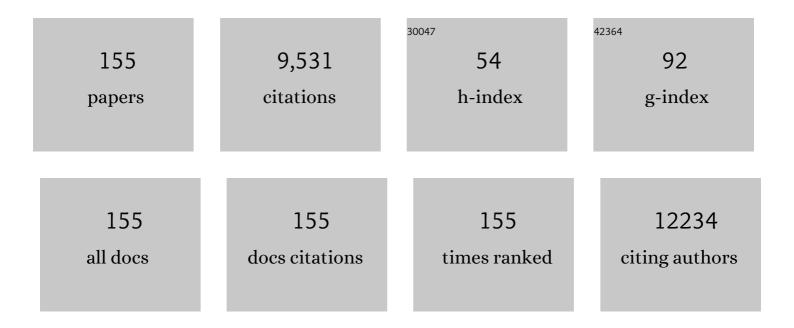


List of Publications by Year in descending order

Source: https://exaly.com/author-pdf/8106425/publications.pdf Version: 2024-02-01



VIDU

#	Article	IF	CITATIONS
1	Two-dimensional metal–organic frameworks with high oxidation states for efficient electrocatalytic urea oxidation. Chemical Communications, 2017, 53, 10906-10909.	2.2	328
2	MoS ₂ /TiO ₂ heterostructures as nonmetal plasmonic photocatalysts for highly efficient hydrogen evolution. Energy and Environmental Science, 2018, 11, 106-114.	15.6	326
3	Bismuth Oxybromide with Reasonable Photocatalytic Reduction Activity under Visible Light. ACS Catalysis, 2014, 4, 954-961.	5.5	300
4	Photocatalytic properties of BiOX (X = Cl, Br, and I). Rare Metals, 2008, 27, 243-250.	3.6	297
5	High-strength scalable MXene films through bridging-induced densification. Science, 2021, 374, 96-99.	6.0	297
6	Three-dimensional controlled growth of monodisperse sub-50 nm heterogeneous nanocrystals. Nature Communications, 2016, 7, 10254.	5.8	267
7	Recent Development of Zeolitic Imidazolate Frameworks (ZIFs) Derived Porous Carbon Based Materials as Electrocatalysts. Advanced Energy Materials, 2018, 8, 1801257.	10.2	242
8	A Yolk–Shell Structured Silicon Anode with Superior Conductivity and High Tap Density for Full Lithiumâ€Ion Batteries. Angewandte Chemie - International Edition, 2019, 58, 8824-8828.	7.2	242
9	Room Temperature Ciant and Linear Magnetoresistance in Topological Insulator <mml:math xmlns:mml="http://www.w3.org/1998/Math/MathML" display="inline"><mml:msub><mml:mi>Bi</mml:mi><mml:mn>2</mml:mn></mml:msub><mml:msub><mml:m Physical Review Letters, 2012, 108, 266806.</mml:m </mml:msub></mml:math 	ni>Te mml</td <td>:mi>≺mml:ra</td>	:mi>≺mml:ra
10	Band-gap engineering of BiOCl with oxygen vacancies for efficient photooxidation properties under visible-light irradiation. Journal of Materials Chemistry A, 2018, 6, 2193-2199.	5.2	232
11	Silicene: A Promising Anode for Lithiumâ€lon Batteries. Advanced Materials, 2017, 29, 1606716.	11.1	179
12	Tuning the Band Gap in Silicene by Oxidation. ACS Nano, 2014, 8, 10019-10025.	7.3	175
13	Superhydrophobic Shape Memory Polymer Arrays with Switchable Isotropic/Anisotropic Wetting. Advanced Functional Materials, 2018, 28, 1705002.	7.8	166
14	Improving the photo-oxidative capability of BiOBr via crystal facet engineering. Journal of Materials Chemistry A, 2017, 5, 8117-8124.	5.2	163
15	High-performance room-temperature sodium–sulfur battery enabled by electrocatalytic sodium polysulfides full conversion. Energy and Environmental Science, 2020, 13, 562-570.	15.6	163
16	Nanodroplets for Stretchable Superconducting Circuits. Advanced Functional Materials, 2016, 26, 8111-8118.	7.8	158
17	Comprehensive New Insights and Perspectives into Tiâ€Based Anodes for Nextâ€Generation Alkaline Metal (Na ⁺ , K ⁺) Ion Batteries. Advanced Energy Materials, 2018, 8, 1801888.	10.2	142
18	Rayleigh-Instability-Induced Bismuth Nanorod@Nitrogen-Doped Carbon Nanotubes as A Long Cycling and High Rate Anode for Sodium-Ion Batteries. Nano Letters. 2019. 19. 1998-2004.	4.5	142

#	Article	IF	CITATIONS
19	Activating Titania for Efficient Electrocatalysis by Vacancy Engineering. ACS Catalysis, 2018, 8, 4288-4293.	5.5	141
20	Thickness-independent scalable high-performance Li-S batteries with high areal sulfur loading via electron-enriched carbon framework. Nature Communications, 2021, 12, 4519.	5.8	139
21	Quasi-freestanding epitaxial silicene on Ag(111) by oxygen intercalation. Science Advances, 2016, 2, e1600067.	4.7	138
22	Realization of flat band with possible nontrivial topology in electronic Kagome lattice. Science Advances, 2018, 4, eaau4511.	4.7	131
23	A 2D metal–organic framework/Ni(OH) ₂ heterostructure for an enhanced oxygen evolution reaction. Nanoscale, 2019, 11, 3599-3605.	2.8	131
24	Modulation of Photocatalytic Properties by Strain in 2D BiOBr Nanosheets. ACS Applied Materials & Interfaces, 2015, 7, 27592-27596.	4.0	130
25	Aqueous Electrolytes with Hydrophobic Organic Cosolvents for Stabilizing Zinc Metal Anodes. ACS Nano, 2022, 16, 9667-9678.	7.3	126
26	A Liquidâ€Metalâ€Based Magnetoactive Slurry for Stimuliâ€Responsive Mechanically Adaptive Electrodes. Advanced Materials, 2018, 30, e1802595.	11.1	106
27	Boron Nitride Nanotubes for Ammonia Synthesis: Activation by Filling Transition Metals. Journal of the American Chemical Society, 2020, 142, 308-317.	6.6	105
28	A Gallium-Based Magnetocaloric Liquid Metal Ferrofluid. Nano Letters, 2017, 17, 7831-7838.	4.5	101
29	Boosting Visible-Light-Driven Photo-oxidation of BiOCl by Promoted Charge Separation via Vacancy Engineering. ACS Sustainable Chemistry and Engineering, 2019, 7, 3010-3017.	3.2	101
30	Recent Progress on Germanene and Functionalized Germanene: Preparation, Characterizations, Applications, and Challenges. Small, 2019, 15, e1805147.	5.2	100
31	Band Gap Modulated by Electronic Superlattice in Blue Phosphorene. ACS Nano, 2018, 12, 5059-5065.	7.3	92
32	A dye-sensitized visible light photocatalyst-Bi24O31Cl10. Scientific Reports, 2014, 4, 7384.	1.6	91
33	Defect Sites-Rich Porous Carbon with Pseudocapacitive Behaviors as an Ultrafast and Long-Term Cycling Anode for Sodium-Ion Batteries. ACS Applied Materials & Interfaces, 2018, 10, 9353-9361.	4.0	91
34	Catalytic pyrolysis of several kinds of bamboos over zeolite NaY. Green Chemistry, 2006, 8, 183-190.	4.6	90
35	A way to enhance the magnetic moment of multiferroic bismuth ferrite. Journal Physics D: Applied Physics, 2010, 43, 242001.	1.3	89
36	Two dimensional bismuth-based layered materials for energy-related applications. Energy Storage Materials, 2019, 19, 446-463.	9.5	89

#	Article	IF	CITATIONS
37	Recent progress on liquid metals and their applications. Advances in Physics: X, 2018, 3, 1446359.	1.5	85
38	Conversion of Intercalated MoO ₃ to Multiâ€Heteroatomsâ€Doped MoS ₂ with High Hydrogen Evolution Activity. Advanced Materials, 2020, 32, e2001167.	11.1	82
39	Boosting Sodium Storage of Doubleâ€5hell Sodium Titanate Microspheres Constructed from 2D Ultrathin Nanosheets via Sulfur Doping. Advanced Materials, 2018, 30, e1804157.	11.1	79
40	Liquid metals and their hybrids as stimulus–responsive smart materials. Materials Today, 2020, 34, 92-114.	8.3	78
41	Monolayer Epitaxial Heterostructures for Selective Visible‣ightâ€Driven Photocatalytic NO Oxidation. Advanced Functional Materials, 2019, 29, 1808084.	7.8	76
42	Cooperative Electron–Phonon Coupling and Buckled Structure in Germanene on Au(111). ACS Nano, 2017, 11, 3553-3559.	7.3	75
43	Honeycomb silicon: a review of silicene. Science Bulletin, 2015, 60, 1551-1562.	4.3	74
44	Promoted Photocharge Separation in 2D Lateral Epitaxial Heterostructure for Visibleâ€Lightâ€Driven CO ₂ Photoreduction. Advanced Materials, 2020, 32, e2004311.	11.1	74
45	Effects of Oxygen Adsorption on the Surface State of Epitaxial Silicene on Ag(111). Scientific Reports, 2014, 4, 7543.	1.6	70
46	Investigation of electron-phonon coupling in epitaxial silicene by <i>in situ</i> Raman spectroscopy. Physical Review B, 2015, 91, .	1.1	67
47	A non-enzymatic photoelectrochemical glucose sensor based on BiVO4 electrode under visible light. Sensors and Actuators B: Chemical, 2019, 291, 34-41.	4.0	67
48	Metal-ion bridged high conductive RGO-M-MoS2 (M = Fe3+, Co2+, Ni2+, Cu2+ and Zn2+) composite electrocatalysts for photo-assisted hydrogen evolution. Applied Catalysis B: Environmental, 2019, 246, 129-139.	10.8	63
49	Finely dispersed Au nanoparticles on graphitic carbon nitride as highly active photocatalyst for hydrogen peroxide production. Catalysis Communications, 2019, 123, 69-72.	1.6	63
50	Nearâ€Infraredâ€Driven Photocatalysts: Design, Construction, and Applications. Small, 2021, 17, e1904107.	5.2	63
51	Photocatalytic Reduction on Bismuth-Based <i>p</i> -Block Semiconductors. ACS Sustainable Chemistry and Engineering, 2018, 6, 15936-15953.	3.2	62
52	Dirac Signature in Germanene on Semiconducting Substrate. Advanced Science, 2018, 5, 1800207.	5.6	59
53	Hydrogen Terminated Germanene for a Robust Selfâ€Powered Flexible Photoelectrochemical Photodetector. Small, 2020, 16, e2000283.	5.2	58
54	Construction of a Bi2MoO6:Bi2Mo3O12 heterojunction for efficient photocatalytic oxygen evolution. Chemical Engineering Journal, 2018, 353, 636-644.	6.6	56

#	Article	IF	CITATIONS
55	In-situ grafting of N-doped carbon nanotubes with Ni encapsulation onto MOF-derived hierarchical hybrids for efficient electrocatalytic hydrogen evolution. Carbon, 2020, 163, 178-185.	5.4	56
56	Binary Pd/amorphous-SrRuO3 hybrid film for high stability and fast activity recovery ethanol oxidation electrocatalysis. Nano Energy, 2020, 67, 104247.	8.2	55
57	Magnetic properties of Bi2FeMnO6: A multiferroic material with double-perovskite structure. Applied Physics Letters, 2010, 97, .	1.5	52
58	Interface Strain-Induced Multiferroicity in a SmFeO ₃ Film. ACS Applied Materials & Interfaces, 2014, 6, 7356-7362.	4.0	52
59	Promoting photoreduction properties via synergetic utilization between plasmonic effect and highly active facet of BiOCl. Nano Energy, 2019, 57, 398-404.	8.2	52
60	Domain wall conductivity in oxygen deficient multiferroic YMnO3 single crystals. Applied Physics Letters, 2011, 99, .	1.5	49
61	The Impacts of Cation Stoichiometry and Substrate Surface Quality on Nucleation, Structure, Defect Formation, and Intermixing in Complex Oxide Heteroepitaxy–LaCrO ₃ on SrTiO ₃ (001). Advanced Functional Materials, 2013, 23, 2953-2963.	7.8	48
62	A ferroelectric photocatalyst Ag ₁₀ Si ₄ O ₁₃ with visible-light photooxidation properties. Journal of Materials Chemistry A, 2016, 4, 10992-10999.	5.2	46
63	Laserâ€Generated Supranano Liquid Metal as Efficient Electron Mediator in Hybrid Perovskite Solar Cells. Advanced Materials, 2020, 32, e2001571.	11.1	46
64	Improving the Photo-Oxidative Performance of Bi ₂ MoO ₆ by Harnessing the Synergy between Spatial Charge Separation and Rational Co-Catalyst Deposition. ACS Applied Materials & Interfaces, 2018, 10, 9342-9352.	4.0	44
65	Lanthanum doped multiferroic DyFeO3: Structural and magnetic properties. Journal of Applied Physics, 2010, 107, .	1.1	43
66	Electronic structure and thermoelectric properties of Bi2Te3 crystals and graphene-doped Bi2Te3. Thin Solid Films, 2010, 518, e57-e60.	0.8	40
67	Au-nanoparticle-supported ZnO as highly efficient photocatalyst for H2O2 production. Catalysis Communications, 2020, 134, 105860.	1.6	39
68	Fe, Cu co-doped BiOBr with improved photocatalytic ability of pollutants degradation. Journal of Alloys and Compounds, 2021, 881, 160391.	2.8	39
69	Galliumâ€based liquid metals for lithiumâ€ion batteries. , 2022, 1, 354-372.		39
70	Unabridged phase diagram for single-phased FeSexTe1-x thin films. Scientific Reports, 2014, 4, 7273.	1.6	38
71	Germanium Nanosheets with Dirac Characteristics as a Saturable Absorber for Ultrafast Pulse Generation. Advanced Materials, 2021, 33, e2101042.	11.1	38
72	Delocalized Surface State in Epitaxial Si(111) Film with Spontaneous â^š3 × â^š3 Superstructure. Scie Reports, 2015, 5, 13590.	ntific 1.6	37

5

#	Article	IF	CITATIONS
73	Observation of van Hove Singularities in Twisted Silicene Multilayers. ACS Central Science, 2016, 2, 517-521.	5.3	37
74	s-p orbital hybridization: a strategy for developing efficient photocatalysts with high carrier mobility. Science Bulletin, 2018, 63, 465-468.	4.3	37
75	Progress and perspectives of bismuth oxyhalides in catalytic applications. Materials Today Physics, 2021, 16, 100294.	2.9	37
76	Depth-profiling of Yb ³⁺ sensitizer ions in NaYF ₄ upconversion nanoparticles. Nanoscale, 2017, 9, 7719-7726.	2.8	36
77	Selective Ferroelectric BiOI/Bi ₄ Ti ₃ O ₁₂ Heterostructures for Visible Light-Driven Photocatalysis. Journal of Physical Chemistry C, 2019, 123, 517-525.	1.5	36
78	Point defects in epitaxial silicene on Ag(111) surfaces. 2D Materials, 2016, 3, 025034.	2.0	35
79	General Synthetic Strategy for Pomegranate-like Transition-Metal Phosphides@N-Doped Carbon Nanostructures with High Lithium Storage Capacity. , 2019, 1, 265-271.		35
80	Synthesis of Multilayer Silicene on Si(111)â^š3 × â^š3-Ag. Journal of Physical Chemistry C, 2017, 121, 27182-27190.	1.5	34
81	Manipulation of domain wall mobility by oxygen vacancy ordering in multiferroic YMnO3. Physical Chemistry Chemical Physics, 2013, 15, 20010.	1.3	32
82	Enhanced Photocatalytic Activity of Bi 24 O 31 Br 10 : Constructing Heterojunction with BiOI. Journal of Materials Science and Technology, 2017, 33, 281-284.	5.6	31
83	Construction of 2D lateral pseudoheterostructures by strain engineering. 2D Materials, 2017, 4, 025102.	2.0	31
84	Highly nonlinear BiOBr nanoflakes for hybrid integrated photonics. APL Photonics, 2019, 4, .	3.0	31
85	Atomically dispersed S-Fe-N4 for fast kinetics sodium-sulfur batteries via a dual function mechanism. Cell Reports Physical Science, 2021, 2, 100531.	2.8	31
86	Boosting NIR-driven photocatalytic water splitting by constructing 2D/3D epitaxial heterostructures. Journal of Materials Chemistry A, 2019, 7, 13629-13634.	5.2	30
87	Indirect-Direct Band Transformation of Few-Layer BiOCl under Biaxial Strain. Journal of Physical Chemistry C, 2016, 120, 8589-8594.	1.5	29
88	Efficient Photocatalytic Hydrogen Peroxide Production over TiO2 Passivated by SnO2. Catalysts, 2019, 9, 623.	1.6	29
89	Fabrication, magnetic, and ferroelectric properties of multiferroic BiFeO3 hollow nanoparticles. Journal of Applied Physics, 2011, 109, .	1.1	28
90	Efficient visible-light photocatalysts by constructing dispersive energy band with anisotropic p and s-p hybridization states. Current Opinion in Green and Sustainable Chemistry, 2017, 6, 93-100.	3.2	28

#	Article	IF	CITATIONS
91	Role of Charge Density Wave in Monatomic Assembly in Transition Metal Dichalcogenides. Advanced Functional Materials, 2019, 29, 1900367.	7.8	28
92	General Programmable Growth of Hybrid Core–Shell Nanostructures with Liquid Metal Nanodroplets. Advanced Materials, 2021, 33, e2008024.	11.1	28
93	Reversible Oxidation of Blue Phosphorus Monolayer on Au(111). Nano Letters, 2019, 19, 5340-5346.	4.5	27
94	Gallium–Indium–Tin Liquid Metal Nanodroplet-Based Anisotropic Conductive Adhesives for Flexible Integrated Electronics. ACS Applied Nano Materials, 2021, 4, 550-557.	2.4	27
95	Optimization of photocarrier dynamics and activity in phosphorene with intrinsic defects for nitrogen fixation. Journal of Materials Chemistry A, 2020, 8, 20570-20580.	5.2	26
96	Application of Scanning Tunneling Microscopy in Electrocatalysis and Electrochemistry. Electrochemical Energy Reviews, 2021, 4, 249-268.	13.1	26
97	Atomic Structural Evolution of Single‣ayer Pt Clusters as Efficient Electrocatalysts. Small, 2021, 17, e2100732.	5.2	26
98	Enhancement of charge separation in ferroelectric heterogeneous photocatalyst Bi ₄ (SiO ₄) ₃ /Bi ₂ SiO ₅ nanostructures. Dalton Transactions, 2017, 46, 15582-15588.	1.6	25
99	Realization of Strained Stanene by Interface Engineering. Journal of Physical Chemistry Letters, 2019, 10, 1558-1565.	2.1	25
100	Fabrication and characterization of textured Bi2Te3 thermoelectric thin films prepared on glass substrates at room temperature using pulsed laser deposition. Journal of Crystal Growth, 2013, 362, 247-251.	0.7	24
101	The origin of enhanced photocatalytic activities of hydrogenated TiO ₂ nanoparticles. Dalton Transactions, 2017, 46, 10694-10699.	1.6	24
102	The Dependence of Bi ₂ MoO ₆ Photocatalytic Water Oxidation Capability on Crystal Facet Engineering. ChemPhotoChem, 2019, 3, 1246-1253.	1.5	23
103	Kondo Holes in the Two-Dimensional Itinerant Ising Ferromagnet Fe ₃ GeTe ₂ . Nano Letters, 2021, 21, 6117-6123.	4.5	23
104	Controlled hydrogenation into defective interlayer bismuth oxychloride via vacancy engineering. Communications Chemistry, 2020, 3, .	2.0	22
105	Wearable Piezoelectric Nanogenerators Based on Core–Shell Ga-PZT@GaO _{<i>x</i>} Nanorod-Enabled P(VDF-TrFE) Composites. ACS Applied Materials & Interfaces, 2022, 14, 7990-8000.	4.0	21
106	Facile synthesis of g-C3N4/BiOClxl1-x hybrids with efficient charge separation for visible-light photocatalysis. Ceramics International, 2020, 46, 10843-10850.	2.3	20
107	Germanene Nanosheets: Achieving Superior Sodiumâ€lon Storage via Pseudointercalation Reactions. Small Structures, 2021, 2, 2100041.	6.9	20
108	Recent Progress on Twoâ€Dimensional Heterostructures for Catalytic, Optoelectronic, and Energy Applications. ChemElectroChem, 2019, 6, 2841-2851.	1.7	18

#	Article	IF	CITATIONS
109	Oxygen-vacancy effect on structural, magnetic, and ferroelectric properties in multiferroic YMnO3 single crystals. Journal of Applied Physics, 2012, 111, .	1.1	17
110	Van der Waals integration of silicene and hexagonal boron nitride. 2D Materials, 2019, 6, 035001.	2.0	17
111	Large-Gap Quantum Spin Hall State and Temperature-Induced Lifshitz Transition in Bi ₄ Br ₄ . ACS Nano, 2022, 16, 3036-3044.	7.3	17
112	Electronic Band Engineering in Elemental 2D Materials. Advanced Materials Interfaces, 2018, 5, 1800749.	1.9	16
113	Pressure Engineering for Extending Spectral Response Range and Enhancing Photoelectric Properties of Iodine. Advanced Optical Materials, 2021, 9, 2101163.	3.6	16
114	Application of organic-inorganic hybrids in lithium batteries. Materials Today Physics, 2020, 15, 100289.	2.9	15
115	The magnetic structure of an epitaxial BiMn0.5Fe0.5O3 thin film on SrTiO3 (001) studied with neutron diffraction. Applied Physics Letters, 2012, 101, .	1.5	14
116	Enhanced energy transfer in heterogeneous nanocrystals for near infrared upconversion photocurrent generation. Nanoscale, 2017, 9, 18661-18667.	2.8	14
117	Roles of Cocatalysts on BiVO ₄ Photoanodes for Photoelectrochemical Water Oxidation: A Minireview. Energy & Fuels, 2022, 36, 11394-11403.	2.5	14
118	Role of Atomic Interaction in Electronic Hybridization in Two-Dimensional Ag ₂ Ge Nanosheets. Journal of Physical Chemistry C, 2017, 121, 16754-16760.	1.5	13
119	Direct cation exchange of surface ligand capped upconversion nanocrystals to produce strong luminescence. Chemical Communications, 2018, 54, 9587-9590.	2.2	13
120	Control of Photocarrier Separation and Recombination at Bismuth Oxyhalide Interface for Nitrogen Fixation. Journal of Physical Chemistry Letters, 2020, 11, 9304-9312.	2.1	13
121	Recent Progress on 2D Kagome Magnets: Binary T <i>_m</i> Sn <i>_n</i> (T = Fe,) Tj ETQo	1 1 0.784 1.8	¦314 rgBT /○ 13
122	Enhanced magnetic moment in ErMnO ₃ by copper doping and negative magnetocapacitance effect. Journal Physics D: Applied Physics, 2010, 43, 325002.	1.3	12
123	Magnetic and ferroelectric properties of multiferroic Bi2NiMnO6 nanoparticles. Journal of Applied Physics, 2011, 109, .	1.1	12
124	New monatomic layer clusters for advanced catalysis materials. Science China Materials, 2019, 62, 149-153.	3.5	12
125	Experimental Realization of Two-Dimensional Buckled Lieb Lattice. Nano Letters, 2020, 20, 2537-2543.	4.5	12
126	Epitaxial Growth of Quasi-One-Dimensional Bismuth-Halide Chains with Atomically Sharp Topological Non-Trivial Edge States. ACS Nano, 2021, 15, 14850-14857.	7.3	12

#	Article	IF	CITATIONS
127	Magnetic properties and microstructures of iron oxide@mesoporous silica core-shell composite for applications in magnetic dye separation. Journal of Applied Physics, 2012, 111, 07B301.	1.1	10
128	Evidence for the dynamic relaxation behavior of oxygen vacancies in Aurivillius Bi2MoO6 from dielectric spectroscopy during resistance switching. Journal of Materials Chemistry C, 2019, 7, 8915-8922.	2.7	10
129	Electric-Field-Driven Negative Differential Conductance in 2D van der Waals Ferromagnet Fe ₃ GeTe ₂ . Nano Letters, 2021, 21, 9233-9239.	4.5	10
130	Pauli-limited effect in the magnetic phase diagram of FeSe <i>x</i> Te1â^' <i>x</i> thin films. Applied Physics Letters, 2015, 107, .	1.5	9
131	Metal–silicene interaction studied by scanning tunneling microscopy. Journal of Physics Condensed Matter, 2016, 28, 034002.	0.7	9
132	Spatial Scales of Heavy Meiyu Precipitation Events in Eastern China and Associated Atmospheric Processes. Geophysical Research Letters, 2020, 47, e2020GL087086.	1.5	9
133	Moiréâ€Potentialâ€Induced Band Structure Engineering in Graphene and Silicene. Small, 2021, 17, e1903769.	5.2	9
134	Anisotropy of crystal growth mechanisms, dielectricity, and magnetism of multiferroic Bi2FeMnO6 thin films. Journal of Applied Physics, 2013, 113, 17D904.	1.1	8
135	Ultra-thin Ga nanosheets: analogues of high pressure Ga(<scp>iii</scp>). Nanoscale, 2019, 11, 17201-17205.	2.8	7
136	Native Surface Oxides Featured Liquid Metals for Printable Self-Powered Photoelectrochemical Device. Frontiers in Chemistry, 2019, 7, 356.	1.8	6
137	Theoretical insights into nitrogen oxide activation on halogen defect-rich {001} facets of bismuth oxyhalide. Journal of Materials Science and Technology, 2021, 77, 217-222.	5.6	6
138	First-principles study on the electronic structures and diffusion behaviors of intrinsic defects in BiOCl. Computational Materials Science, 2022, 203, 111088.	1.4	6
139	Facet-dependent Electronic Quantum Diffusion in the High-Order Topological Insulator <mml:math xmlns:mml="http://www.w3.org/1998/Math/MathML" display="inline" overflow="scroll"><mml:msub><mml:mi>Bi</mml:mi><mml:mn>4</mml:mn></mml:msub><mml:msub><mml:msub><mml:mi< td=""><td>>Br<td>:mi><mml:n< td=""></mml:n<></td></td></mml:mi<></mml:msub></mml:msub></mml:math 	>Br <td>:mi><mml:n< td=""></mml:n<></td>	:mi> <mml:n< td=""></mml:n<>
140	Reversible Potassium Intercalation in Blue Phosphorene–Au Network Driven by an Electric Field. Journal of Physical Chemistry Letters, 2020, 11, 5584-5590.	2.1	5
141	Reconstructing the Surface Structure of NaREF ₄ Upconversion Nanocrystals with a Novel K ⁺ Treatment. Chemistry of Materials, 2021, 33, 2548-2556.	3.2	5
142	Epitaxial growth of bilayer Bi(110) on two-dimensional ferromagnetic Fe ₃ GeTe ₂ . Journal of Physics Condensed Matter, 2022, 34, 074003.	0.7	5
143	Role of surface wettability in photoelectrocatalytic oxygen evolution reactions. Materials Today Energy, 2022, 25, 100961.	2.5	5
144	Resolving the intrinsic bandgap and edge effect of BiI3 film epitaxially grown on graphene. Materials Today Physics, 2021, 20, 100454.	2.9	4

#	Article	IF	CITATIONS
145	Boosting Lightâ€Ðriven Photocatalytic Water Splitting of Bi ₄ NbO ₈ Br by Polarization Field. Solar Rrl, 2022, 6, .	3.1	4
146	Effects of Cu and Fe doping on Raman spectra and on the structural and magnetic properties of ErMnO3. Journal of Applied Physics, 2011, 109, 07D710.	1.1	3
147	Magnetostrictive properties of directional solidification Fe82Ga9Al9 alloy. Journal of Applied Physics, 2012, 111, 07A332.	1.1	3
148	Simulation study on horizontal continuous casting process of copper hollow billet under rotating electromagnetic stirring Part 2—effects of electromagnetic and casting parameters on solidification process. Materials Science and Technology, 2011, 27, 684-692.	0.8	2
149	Raman Studies on Silicene and Germanene. Surface Innovations, 0, , 1-31.	1.4	2
150	High Pressure Driven Isostructural Electronic Phase Separation in 2D BiOI. Physica Status Solidi - Rapid Research Letters, 2019, 13, .	1.2	2
151	Adsorption of Molecules on Silicene. Springer Series in Materials Science, 2016, , 215-242.	0.4	1
152	BiOBr nanoflakes with strong Kerr nonlinearity towards hybrid integrated photonic devices. , 2020, , .		1
153	Defects in two-dimensional elemental materials beyond graphene. , 2022, , 43-88.		1
154	Thickness tunable Kerr nonlinearity in BiOBr nanoflakes. , 2020, , .		0
155	Technical evolution for the identification of Xenes: from microscopy to spectroscopy. , 2022, , 225-254.		0